Silanes

DOI: 10.1002/ange.200502527

An η^3-H_2SiR_2 Adduct of [{PhB-(CH_2PiPr_2)$_3$}$Fe^{II}H$]**

*Christine M. Thomas and Jonas C. Peters**

The tripodal tris(phosphino)borate ligand $[PhB(CH_2PiPr_2)_3]^-$ (abbreviated $[PhBP^{iPr}_3]$) stabilizes iron complexes in a wide range of oxidation states, including high-valent Fe^{IV}.[1] $[(PhBP^{iPr}_3)FeL_n]$ systems are, moreover, known to mediate a

[*] C. M. Thomas, Professor J. C. Peters
Division of Chemistry and Chemical Engineering
Arnold and Mabel Beckman Laboratories of Chemical Synthesis
California Institute of Technology
Pasadena, CA 91125 (USA)
Fax: (+1) 626-577-4088
E-mail: jpeters@caltech.edu.

[**] This work was supported by the NSF (CHE-01232216) and BP (MC^2 program). Larry Henling and Dr. Mike Day are acknowledged for crystallographic assistance, and Erin J. Daida is acknowledged for executing several preliminary screen reactions. We also thank the referees of this manuscript for several insightful suggestions.

Supporting information for this article is available on the WWW under http://www.angewandte.org or from the author.

number of two-electron redox transformations, including Fe^{II}/Fe^{IV} oxidative group transfer and oxidative addition/reductive elimination processes.[1a,c] In the latter context, it was recently demonstrated that four-coordinate iron alkyl species of the type $[(PhBP^{iPr}_3)Fe^{II}R]$ undergo facile hydrogenolysis to generate iron(IV) trihydrides of the type $[(PhBP^{iPr}_3)Fe^{IV}(H)_3(PR_3)]$ that can be likewise generated by H_2 addition to $[(PhBP^{iPr}_3)Fe^{II}(H)(PR_3)]$ precursors.[1c] These complexes mediate catalytic olefin hydrogenation, most likely through uncommon Fe^{II}/Fe^{IV} oxidative addition/reductive elimination steps.[1c] Motivated by these findings, we have examined the reactivity of these four-coordinate $[(PhBP^{iPr}_3)Fe^{II}R]$ alkyl species with silane substrates for comparison with their reactivity towards H_2, anticipating that structurally distinctive iron silylene species might be generated. Herein, we report the structural and spectroscopic characterization of unusual η^3-silane adducts of iron(II), namely $[(PhBP^{iPr}_3)Fe^{II}(H)(\eta^3\text{-}H_2SiR_2)]$. As described below, the available structural, spectroscopic, and theoretical data also suggest the possibility that the $[(PhBP^{iPr}_3)Fe^{II}(H)(\eta^3\text{-}H_2SiR_2)]$ systems described herein equilibrate via silylene intermediates of the type $[(PhBP^{iPr}_3)Fe^{IV}(H)_3(SiR_2)]$.[2] Such silylene intermediates would be isoelectronic with the previously reported $[(PhBP^{iPr}_3)Fe^{IV}(H)_3(PR_3)]$ but appear to be too high in energy relative to their ground state $[(PhBP^{iPr}_3)Fe^{II}(H)(\eta^3\text{-}H_2SiR_2)]$ isomers to be directly observed.

Although silicon-containing transition-metal complexes that exhibit η^2-$HSiR_3$ interactions are ubiquitous,[3,4] those that exhibit well-characterized interactions between two or more metal hydrides and a coordinated silicon atom are much less common. These interactions have nevertheless been described in certain cases, such as in the dinuclear complex $[\{(PR_3)_2(H)_2Ru\}_2(\eta^4\text{-}SiH_4)]$ of Sabo-Etienne and co-workers[5] and in the mononuclear complexes $[ReH_4(PPh_3)(\eta^3\text{-}H_2SiR_3)]$,[6] $[(PCy_3)_2Ru(H)(\eta^2\text{-}H_2)(\eta^3\text{-}H_2SiPh_3)]$ (Cy = cyclohexyl),[7] $[Ru(PPh_3)_3H_3SiMeCl_2]$,[8] and $[Cp^*Ru(PPh_3)(\eta^3\text{-}H_2SiMeCl_2)]$ ($Cp^* = C_5Me_5$).[9] Metal hydride/silyl systems of these types are often described as lying somewhere along the continuum to oxidative addition, the limit being full oxidative addition with earlier, "arrested" addition stages also being common.[4a] To the best of our knowledge, the $[(PhBP^{iPr}_3)Fe^{II}(H)(\eta^3\text{-}H_2SiR_2)]$ complexes described here are the first thoroughly characterized examples of arrested silane adducts of iron that exhibit an η^3 binding mode (i.e., $Fe(\eta^3\text{-}H_2SiR_2)$). The only other example of this binding mode for a silane ligand of any transition-metal complex appears to be the aforementioned dinuclear ruthenium system of Sabo-Etienne.[5]

A $[(PhBP^{iPr}_3)Fe^{II}(H)(\eta^3\text{-}H_2SiR_2)]$ species is formed by the reaction between $[(PhBP^{iPr}_3)FeMe]$ (**1**) and $PhSiH_3$ (Scheme 1), which leads to the quantitative formation of a single diamagnetic red product (**2**), as evidenced by ^{1}H NMR spectroscopy. In contrast to the previously reported reaction of **1** with H_2,[1c] no

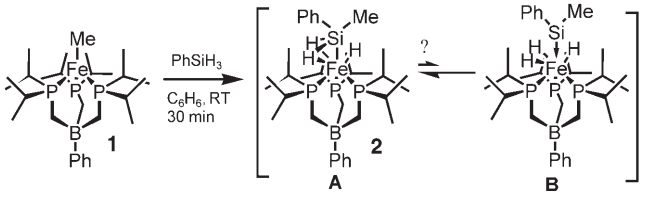

Scheme 1. Reaction of **1** with phenylsilane.

methane loss is detected by ^{1}H NMR spectroscopy. The $^{31}P\{^1H\}$ NMR spectrum of **2** reveals a broad singlet at $\delta = 76$ ppm, which is consistent with a C_{3v}-symmetric structure. All three phosphorus nuclei remain magnetically equivalent in the $^{31}P\{^1H\}$ NMR spectrum at temperatures as low as $-80\,^\circ$C. The ^{1}H NMR spectrum of **2** reveals a hydride signal at $\delta = -13.5$ ppm with a complicated splitting pattern (see below).

To assess the structure of complex **2** in the solid state, X-ray quality single crystals were grown by cooling a concentrated solution of **2** in diethyl ether to $-35\,^\circ$C. High-resolution X-ray diffraction analysis provided the solid-state structure shown in Figure 1.[10] The structure confirms that a 1,2-methyl migration occurs from the iron center to the silicon center during the transformation. A remarkably short Fe···Si distance of 2.1280(7) Å is present that is very similar to the Fe···Si distance of 2.154(1) Å reported for the only structurally characterized example of an iron silylene species, $[Cp^*Fe(CO)(SiMes_2)SiMe_3]$ ($Mes = 2,4,6\text{-}Me_3C_6H_2$).[11] Moreover, the geometry of the silicon atom of **2** is rigorously

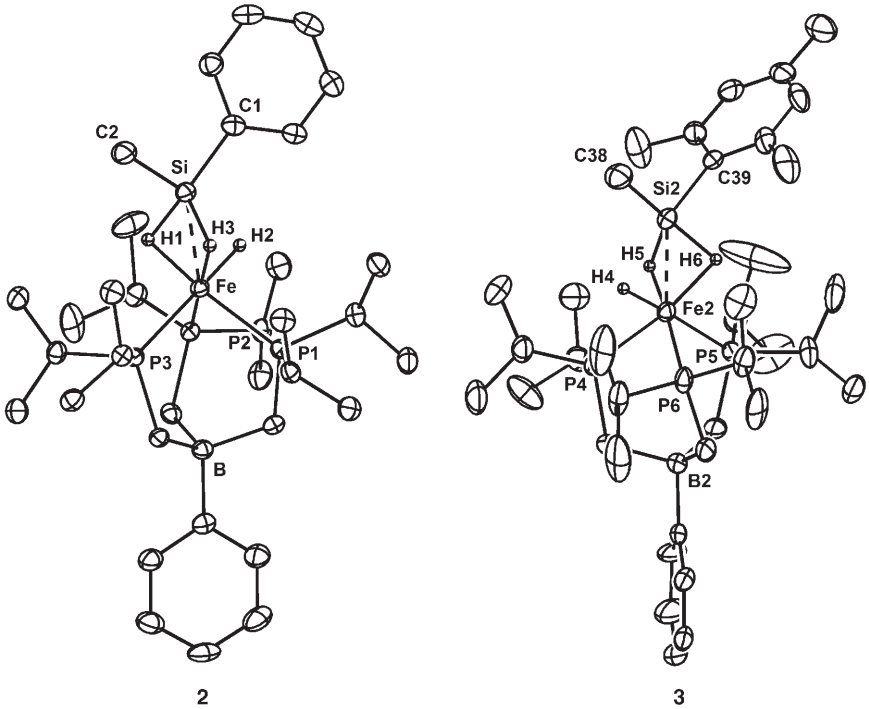

Figure 1. Solid-state molecular structure of $[(PhBP^{iPr}_3)Fe^{II}(H)(H_2SiPhMe)]$ (**2**) and $[(PhBP^{iPr}_3)Fe^{II}(H)(H_2SiMesMe)]$ (**3**) showing 50% displacement ellipsoids. Only one of the two independent molecules present in the asymmetric unit of **3** is shown. Hydrogen atoms other than the hydrides of interest have been omitted for clarity.

planar (∢C2-Si-Fe + ∢C2-Si-C1 + ∢C1-Si-Fe = 360°) if one considers its connectivity to the phenyl, methyl, and iron substituents only. These structural data suggested a Si atom with silylene character and led to our initial, but ultimately incorrect, assignment of **2** as a silylene trihydride of structure type **B** (Scheme 1). All three hydride positions could be located in the difference Fourier map and refined, and careful examination reveals that two of the hydrides (H1 and H3) are located within bonding distance of both the iron and the silicon centers (Fe–H1: 1.55 Å; Fe–H3: 1.57 Å; Si–H1: 1.46 Å; Si–H3: 1.55 Å). The third hydride (H2) is located outside the typical bonding radius of the silicon atom (2.00 Å)[4b] and resides appreciably closer to the Fe center (Fe–H2: 1.48 Å). These data are inconsistent with the silylene structure **B**.

As there is inevitable uncertainty in accurately locating the positions of hydrogen atoms close to much heavier atoms such as Si and Fe by X-ray crystallography, a related complex was prepared for additional structural support of the assignment. In an analogous reaction to that shown in Scheme 1, complex **1** reacts with one equivalent of mesitylsilane (H_3SiMes) to generate a diamagnetic red product (**3**) in quantitative yield. Complex **3** displays analogous NMR data to that of **2**, with a $^{31}P\{^1H\}$ shift at $\delta = 79$ ppm and a hydride-type ^1H NMR resonance at $\delta = -13.4$ ppm, which also suggests a highly symmetric structure in solution. X-ray quality crystals could be obtained in a similar way, and one of the two independent molecules present in the asymmetric unit is shown in Figure 1.[12] As in the case of **2**, two of the three hydrides are located within bonding distance of the silicon atom in each molecule (Si–H5: 1.56 and 1.62 Å; Si–H6: 1.67 and 1.74 Å), while the third hydride appears to be outside the bonding radius of the Si atom (Si···H4: 2.14 and 1.97 Å). The Fe···Si distances in both molecules for **3** (2.131(1) and 2.141(1) Å) are essentially identical to that in **2** (2.1280(7) Å). Regardless of the inevitable uncertainty in the specific Fe···H and Si···H distances, the significant similarity between the structures of **2** and **3** strongly suggests the presence of two 3-centered Fe-H-Si interactions in the solid state and one Fe-H(hydride) interaction.

For additional structural examination of the hydride positions, a density functional (DFT) geometry optimization of the structure of **2** was performed using the Jaguar package (B3LYP/LACVP**).[13,14] All of the atoms of **2** were used in the calculation, and the structure was minimized using the experimentally determined crystallographic coordinates as an initial estimate. The resulting Fe–H and Si–H bond lengths were very similar to those determined by crystallography (Table 1). Interestingly, perturbing the crystallographic coordinates to provide a more threefold symmetric structure without Si-H interactions as a starting point led to the same structural minimum. It is gratifying to note that the DFT model locates two short and one much longer Si···H distance, which is in accord with the η^3-H_2SiR_2 adduct formulation. Accordingly, a natural bond orbital (NBO) analysis predicts only two Si–H bonding orbitals (Si–H1, Si–H3).[15] Likewise, only one Fe–H bonding orbital is predicted (Fe–H2) and no bonding orbital is located between Si and Fe. The cutoff energy for locating a bond for donor–acceptor-type interactions is less than 20 kJ mol^{-1}. Interactions below this energy are ignored by NBO analaysis.[13,15] Therefore, the experimentally observed close contact between the iron center and the silicon–hydride bonds Si–H1 and Si–H3 is best characterized as η^3 in character. Likewise, any interaction between the iron hydride H2 and the Si center would also be characterized as an attractive interaction, although likely one of a much weaker nature if it is present at all. Complexes **2** and **3** are therefore best described as η^3 silane adducts of an iron(II) hydride (structure type **A** in Scheme 1) and not as iron(IV) silylene trihydrides (structure type **B**).

Table 1: Interatomic distances for **2** as determined by X-ray crystallography and a DFT (B3LYP/LACVP**) geometry optimization.

	Experimental [Å]	Calculated [Å]
Fe–Si	2.1280(7)	2.166
Fe–H1	1.553(1)	1.555
Fe–H2	1.482(1)	1.484
Fe–H3	1.566(2)	1.569
Si–H1	1.464(1)	1.469
Si–H2	2.001(2)	2.073
Si–H3	1.552(2)	1.554

Further inspection of the solution-state NMR data available for **2** confirms that a significant Si···H interaction is also maintained in the solution phase. A $T_{1\,min}$ measurement of 177 ms (−30 °C, [D_8]toluene) was determined for the hydride resonance of the ^1H NMR spectrum. This large value would appear to rule out the presence of a nonclassical dihydrogen adduct species (η^2-H_2) but does not help to distinguish between a classical hydride formulation versus the η^2-Si–H–Fe interaction suggested by the crystallographic and DFT data.[16,17] Simulation of the hydride signal (Figure 2) reveals that its complicated splitting pattern arises from first-order coupling of each equivalent hydride to one *trans* phosphorus atom ($^2J_{P\text{-}H} = 27$ Hz) and two *cis* phosphorus atoms ($^2J_{P\text{-}H} = 3$ Hz). The coupling pattern is complicated by second-order effects that result from phosphorus–phosphorus coupling ($^2J_{P\text{-}P} = 62$ Hz). Accordingly, the hydride signal appears as a singlet in the $^1H\{^{31}P\}$ NMR spectrum. The second-order splitting pattern of the hydride signal in the

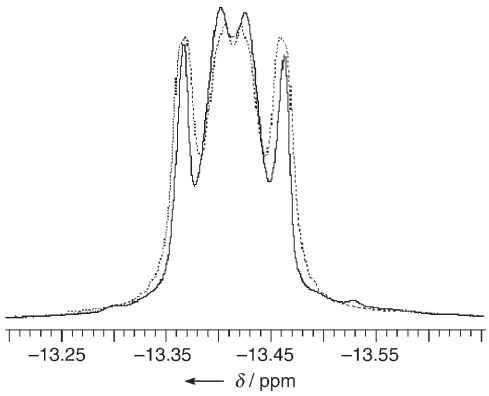

Figure 2. Experimental (solid) and simulated (dotted) ^1H NMR spectrum of **2** (500 MHz, 25 °C, C_6D_6) in the hydride region. See text for discussion.

^{1}H NMR spectrum changes as the temperature of the solution decreases, which indicates a fluxional process of some type (see Supporting Information). Decoalescence of the signal, however, likely occurs at temperatures well below those examined (−80 °C).

The ^{29}Si{^{1}H} NMR data obtained for **2** and **3** reveal signals at $\delta = 162$ and 160 ppm,[18] respectively. These values are significantly downfield of known classical transition-metal–silyl adducts ($\delta = -120$ to 90 ppm) but are also upfield of reported transition-metal silylenes ($\delta = > 200$ ppm).[4a,2] Although monomeric complexes containing η^2-HSiR$_3$ interactions display a wide range of chemical shifts in the ^{29}Si{^{1}H} NMR spectrum (from $\delta = -28$ to 55 ppm),[3,4a] the unusually large downfield shifts observed for **2** and **3** are likely reflective of the η^3 nature of the silane ligand and the very close Fe–Si contact that results, as evident from the solid-state structures.

Closer inspection of the hydride signals for both **2** and **3** reveals the presence of ^{29}Si satellites that provide $J_{\text{Si-H}}$ coupling values of 68 and 70 Hz, respectively. The rapid exchange of the hydrides in solution means that the actual ^{29}Si coupling can be determined by the following equation: $J_{\text{obs}} = 1/3[2\times {}^1J_{\text{Si-H}(\eta^2)} + {}^2J_{\text{Si-H(terminal)}}]$.[19] If it is assumed that $^2J_{\text{Si-H(terminal)}}$ is zero, maximum $^1J_{\text{Si-H}(\eta^2)}$ values of 102 and 105 Hz are predicted for **2** and **3**, respectively. An HMQC experiment was undertaken for each species to confirm these coupling constants and to assign the solution structures of **2** and **3** definitively.[20] The data reveal a direct correlation between the ^{29}Si NMR signals of **2** and **3** and their corresponding hydride signals in the ^{1}H NMR spectrum (see Supporting Information). These data further confirm that Si–H interactions exist for **2** and **3** both in solution and in the solid state.

On the basis of the structural, spectroscopic, and DFT data, **2** and **3** are assigned as iron(II) hydride complexes featuring two η^2-Si–H interactions that give rise to η^3-H$_2$SiR$_2$ adducts of [(PhBP$^{i\text{Pr}}_3$)Fe$^{\text{II}}$H]. Although a third, very weak attractive interaction with the hydride ligand cannot be fully dismissed,[4d] such an interaction would need to be regarded as highly distinct from that of the other two H atoms, in which a strong interaction with both Si and Fe is evident. Whereas three-centered, two-electron bonding interactions in **2** and **3** are apparent in their solid-state structures, all three hydrides undergo rapid exchange in solution and appear to be chemically equivalent. It seems plausible to us that an iron(IV) silylene trihydride, shown as structure type **B** in Scheme 1, could be responsible for the rapid interconversion of the hydride positions on the NMR time scale. As noted above, isolobal [(PhBP$^{i\text{Pr}}_3$)Fe$^{\text{IV}}$(H)$_3$(PR$_3$)] species are chemically stable within this system, and the extremely short Fe–Si bond length, together with the planar nature around the Si center with respect to the methyl, phenyl, and iron substituents, suggests that virtually no structural reorganization would be required at the Si center under such a scenario. An alternative mechanism for interconversion concerns an intermediate in which the Si center interacts equivalently with all three H atoms. This would give rise to a [(PhBP$^{i\text{Pr}}_3$)Fe(η^4-H$_3$SiR$_2$)] intermediate. The possibility of a weak interaction between the Si center and the hydride ligand in the ground-state structures of **2** and **3** would set the stage for this type of dynamic pathway.[3g]

Likewise, a number of mechanistic pathways to account for the overall formation of **2** and **3** can be envisioned. Two plausible mechanisms are shown in Scheme 2. In view of the propensity for the [PhBP$^{i\text{Pr}}_3$]Fe scaffold to undergo two-

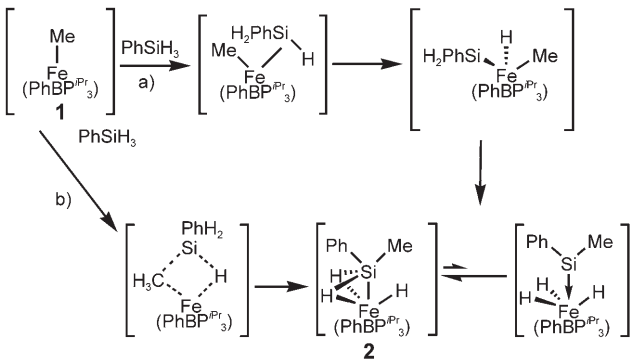

Scheme 2. Two possible mechanisms for the formation of **2**.

electron redox processes, it is perhaps most reasonable to propose an oxidative addition/reductive elimination mechanism as shown in path a.[1] In this scenario, the first step is coordination of silane followed by an oxidative addition to the Fe$^{\text{II}}$ center. Reductive 1,2-methyl migration from iron to silicon then affords an isomer of **2** (or **3**). A sigma-bond metathesis (pathway b) also provides a convenient and potentially low energy methyl-migration pathway. No intermediates could be detected when the reaction between **1** and PhSiH$_3$ was monitored by ^{1}H NMR spectroscopy at low temperature (−50 °C, [D$_8$]toluene).

Methane loss does not occur during the course of the reaction between **1** and phenylsilane or mesitylsilane, whereas such loss occurs readily when **1** is exposed to H$_2$.[1c] To probe the possibility that reversible methane loss and reactivation might be occurring prior to methyl migration, a deuterium-labeling study was undertaken. The deuterated methyl species, [(PhBP$^{i\text{Pr}}_3$)FeCD$_3$] ([CD$_3$]-**1**), is generated by addition of [D$_3$]MeLi to [(PhBP$^{i\text{Pr}}_3$)FeCl]. Reaction between [CD$_3$]-**1** and PhSiH$_3$ results in the formation of [(PhBP$^{i\text{Pr}}_3$)Fe(H)(H$_2$SiPhCD$_3$)] ([CD$_3$]-**2**) as the sole product, as evidenced by ^{1}H NMR data (see Supporting Information). Likewise, the reaction between **1** and PhSiD$_3$ results in the formation of [(PhBP$^{i\text{Pr}}_3$)Fe(D)(D$_2$SiPhMe)] ([D],[D$_2$-silyl]-**2**). These experiments appear to rule out any incipient methane formation prior to methyl migration.

Finally, **1** exhibits selectivity for primary silane substrates. No reaction is observed between **1** and secondary or tertiary silane substrates (e.g., Ph$_2$SiH$_2$ and Et$_3$SiH) over extended periods, presumably because such silanes cannot lead to the thermodynamically stable η^3-silane adduct structures. Secondary silane substrates do react, however, if **1** is exposed to H$_2$ in their presence. For example, **1** reacts with MePhSiH$_2$ to produce **2** quantitatively under a blanket of hydrogen (Scheme 3). Examination of this reaction sequence at low temperature (−20 °C, [D$_8$]toluene) reveals methane loss and the initial formation of the previously reported trihydride species [(PhBP$^{i\text{Pr}}_3$)FeH$_3$] prior to product formation.[1c] [(PhBP$^{i\text{Pr}}_3$)FeH$_3$] gradually decays as **2** appears. This sequence

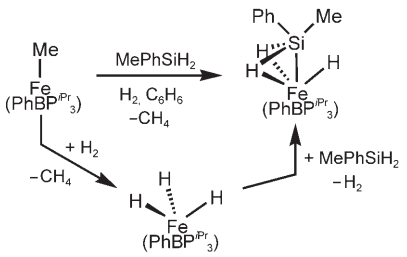

Scheme 3. Reaction of **1** with $MePhSiH_2$ under H_2.

suggests that **1** reacts with H_2 to generate a reactive hydride source that is then trapped by silane, analogous to the trapping of such hydride species by the addition of a phosphine donor.[1c]

In conclusion, it has been found that the [(PhBP$^{iPr}_3$)FeMe] complex reacts with primary aryl silanes to mediate Si–H bond activations and 1,2-methyl migrations that generate unusual η^3-H_2SiRMe silane adducts of [(PhBP$^{iPr}_3$)Fe^{II}H] (R = Ph, Mes). These iron complexes serve as relatives to the numerous Group 8 complexes of the general type [L_3M-(ER_3)H_3] (E = Si, Sn; M = Fe, Ru, Os) now known.[21] The key distinction to be drawn is that the complexes described herein feature a less-substituted Si atom that strongly attracts two Fe–H bonds—resulting in the formation of a [(PhBP$^{iPr}_3$)Fe(H)(η^3-H_2SiR_2)] complex with a very short Fe···Si distance that is distinct from, but closely associated with, its silylene isomer [(PhBP$^{iPr}_3$)Fe(H)$_3$(SiR_2)].

Received: July 19, 2005
Revised: October 12, 2005
Published online: December 21, 2005

Keywords: borates · iron · phosphanes · silanes

[1] a) T. A. Betley, J. C. Peters, *J. Am. Chem. Soc.* **2004**, *126*, 6252; b) T. A. Betley, J. C. Peters, *J. Am. Chem. Soc.* **2003**, *125*, 10782; c) E. J. Daida, J. C. Peters, *Inorg. Chem.* **2004**, *43*, 7474.

[2] For relevant examples of transition-metal–silylene complexes, see: a) J. C. Peters, J. D. Feldman, T. D. Tilley, *J. Am. Chem. Soc.* **1999**, *121*, 9871; b) B. V. Mork, T. D. Tilley, *J. Am. Chem. Soc.* **2004**, *126*, 4385; c) J. D. Feldman, J. C. Peters, T. D. Tilley, *Organometallics* **2002**, *21*, 4065; d) P. B. Glaser, P. W. Wanandi, T. D. Tilley, *Organometallics* **2004**, *23*, 693; e) C. Beddie, M. B. Hall, *J. Am. Chem. Soc.* **2004**, *126*, 13564; f) P. Glaser, T. D. Tilley, *J. Am. Chem. Soc.* **2003**, *125*, 13640.

[3] For examples of Group 8 η^2-silane adducts, see: a) S. C. Bart, E. Lobkovsky, P. J. Chirik, *J. Am. Chem. Soc.* **2004**, *126*, 13794; b) Y. Ohki, T. Kojima, M. Oshima, H. Suzuki, *Organometallics* **2001**, *20*, 2654; c) R. S. Simons, C. A. Tessier, *Organometallics* **1996**, *15*, 2604; d) E. Scharrer, M. Brookhart, *J. Organomet. Chem.* **1995**, *497*, 61; e) U. Schubert, S. Gilbert, S. Mock, *Chem. Ber.* **1992**, *125*, 835; f) E. Scharrer, S. Chang, M. Brookhart, *Organometallics* **1995**, *14*, 5686; g) F. Delpech, S. Sabo-Etienne, J.-C. Daran, B. Chaudret, K. Hussein, C. J. Marsden, J.-C. Barthelat, *J. Am. Chem. Soc.* **1999**, *121*, 6668; h) I. Atheaux, F. Delpech, B. Donnadieu, S. Sabo-Etienne, B. Chaudret, K. Hussein, J.-C. Barthelat, T. Braun, S. B. Duckett, R. N. Perutz, *Organometallics* **2002**, *21*, 5347; i) S. Lachaize, S. Sabo-Etienne, B. Donnadieu, B. Chaudret, *Chem. Commun.* **2003**, 214.

[4] For reviews that cover η^2-Si–H interactions, see: a) J. Y. Corey, J. Braddock-Wilking, *Chem. Rev.* **1999**, *99*, 175; b) U. Schubert, *Adv. Organomet. Chem.* **1990**, *30*, 151; c) G. I. Nikonov, *J. Organomet. Chem.* **2001**, *635*, 24; d) Z. Lin, *Chem. Soc. Rev.* **2002**, *31*, 239; e) G. J. Kubas, *Metal Dihydrogen and Sigma Bond Complexes: Structure, Theory, and Reactivity*, Kluwer Academic, New York, **2001**.

[5] a) I. Atheaux, B. Donnadieu, J.-C. Daran, S. Sabo-Etienne, B. Chaudret, K. Hussein, J.-C. Barthelat, *J. Am. Chem. Soc.* **2000**, *122*, 5664; b) R. Ben Said, K. Hussein, J.-C. Barthelat, I. Atheaux, S. Sabo-Etienne, M. Grellier, B. Donnadieu, B. Chaudret, *Dalton Trans.* **2003**, 4139.

[6] X.-L. Luo, D. Baudry, P. Boydell, P. Charpin, M. Nierlich, M. Ephritikhine, R. H. Crabtree, *Inorg. Chem.* **1990**, *29*, 1511.

[7] K. Hussein, C. J. Marsden, J.-C. Barthelat, V. Rodriguez, S. Conejero, S. Sabo-Etienne, B. Donnadieu, B. Chaudret, *Chem. Commun.* **1999**, 1315.

[8] N. M. Yardy, F. R. Lemke, *Organometallics* **2001**, *20*, 5670.

[9] A. L. Osipov, S. M. Gerdov, L. G. Kuzmina, J. A. K. Howard, G. I. Nikonov, *Organometallics* **2005**, *24*, 587.

[10] Crystallographic data for [(PhBP$^{iPr}_3$)Fe^{II}(H)(H_2SiPhMe)] (**2**): M_r = 660.51, red block, collection temperature = 100 K, triclinic, space group $P\bar{1}$, a = 11.3852(12), b = 12.0036(13), c = 16.1029(17) Å, α = 95.172(2), β = 107.352(2), γ = 95.805(2)°, V = 2072.9(4) Å^3, Z = 2, R_1 = 0.0309 [$I > 2\sigma(I)$], GOF = 1.068. CCDC-273356 (**2**) contains the supplementary crystallographic data for this paper. These data can be obtained free of charge from The Cambridge Crystallographic Data Centre via www.ccdc.cam.ac.uk/data_request/cif.

[11] H. Tobita, A. Matsuda, H. Hashimoto, K. Ueno, H. Ogino, *Angew. Chem.* **2004**, *116*, 223; *Angew. Chem. Int. Ed.* **2004**, *43*, 221.

[12] Crystallographic data for [(PhBP$^{iPr}_3$)Fe(H)(H_2SiMesMe)] (**3**): M_r = 702.59, red block, collection temperature = 100 K, orthorhombic, space group $P2_12_12_1$, a = 18.1126(13), b = 20.3251(14), c = 21.6417(16) Å, V = 7967.2(10) Å^3, Z = 8, R_1 = 0.0609 [$I > 2\sigma(I)$], GOF = 1.677. CCDC-27358 (**3**) contains the supplementary crystallographic data for this paper. These data can be obtained free of charge from The Cambridge Crystallographic Data Centre via www.ccdc.cam.ac.uk/data_request/cif.

[13] Jaguar 5.0, Schrodinger, LLC, Portland, Oregon, 2002.

[14] C. Lee, W. Yang, R. G. Parr, *Phys. Rev. B* **1988**, *37*, 785.

[15] NBO 5.0, E. D. Glendening, J. K. Badenhoop, A. E. Reed, J. E. Carpenter, J. A. Bohmann, C. M. Morales, F. Weinhold, Theoretical Chemistry Institute, University of Wisconsin, Madison, 2001; http://www.chem.wisc.edu/≈nbo5.

[16] R. H. Crabtree, M. Lavin, L. Bonneviot, *J. Am. Chem. Soc.* **1986**, *108*, 4032.

[17] For comparison, the recently reported [(PhBP$^{iPr}_3$)Fe(H)$_3$(PMe_3)] complex exhibits a $T_{1\,min}$ of 140 ms.[1c]

[18] The ^{29}Si{^{1}H} signal for **3** appears as a sharp quartet ($^2J_{Si\text{-}P}$ = 61 Hz) while the signal for **2** is a broad singlet.

[19] F. L. Taw, R. G. Bergman, M. Brookhart, *Organometallics* **2004**, *23*, 886–890.

[20] R. M. Silverstein, F. X. Webster, *The Spectrometric Identification of Organic Compounds*, 6th ed., Wiley, New York, **1998**, chap. 6, pp. 262.

[21] For examples, see: a) S. Gilbert, M. Knorr, S. Mock, U. Schubert, *J. Organomet. Chem.* **1994**, *480*, 241; b) L. J. Procopio, D. H. Berry, *J. Am. Chem. Soc.* **1991**, *113*, 4039; c) C. E. F. Rickard, W. R. Roper, S. D. Woodgate, L. J. Wright, *J. Organomet. Chem.* **2000**, *609*, 177; d) K. Hubler, U. Hubler, W. R. Roper, P. Schwerdtfeger, L. J. Wright, *Chem. Eur. J.* **1997**, *3*, 1608–1616.

